SAND2016-8841C

Exceptional service in the national interest

Sandia National Laboratories

Simulating hydrogen embrittlement and fast pathways for diffusion

James Foulk III, Gabriel de Frias, Jakob Ostien, Alejandro Mota, Waiching Sun (Columbia), Guy Bergel (UC Berkeley)
Collaborators: Bill Wolfer (LLNL), Chris San Marchi, Brian Somerday (SwRI)

- Motivated through observation
- Strong chemo-mechanical coupling
- Capture sub-grid processes through a surface approach
- Explore fast pathways for diffusion at structural and microstructural scales
- Develop models for H/T/He embrittlement w/focus on void nucleation

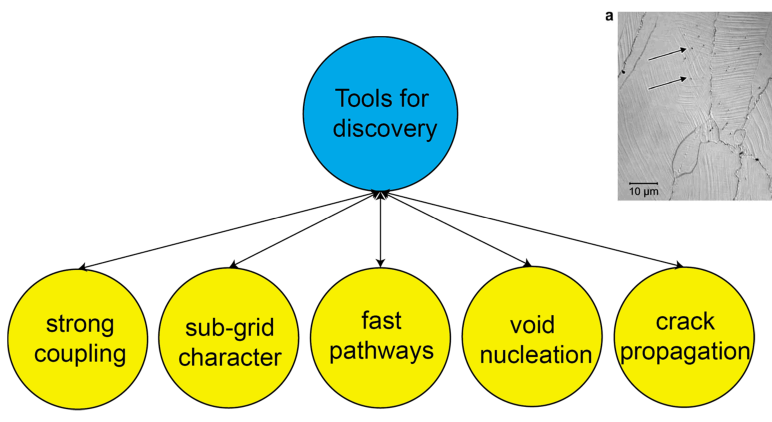

(Nibur, 2009)

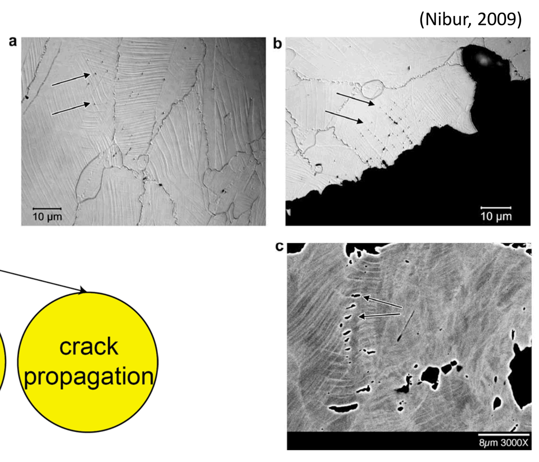

- Compact tension specimens, B ~ 13 mm; W ~ 26 mm
- Constant pressure of gaseous hydrogen: 103 MPa
- "Loading rates" ~ 0.6 - 10 MPa $m^{1/2}$ per minute

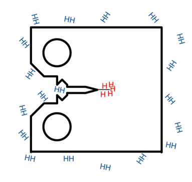

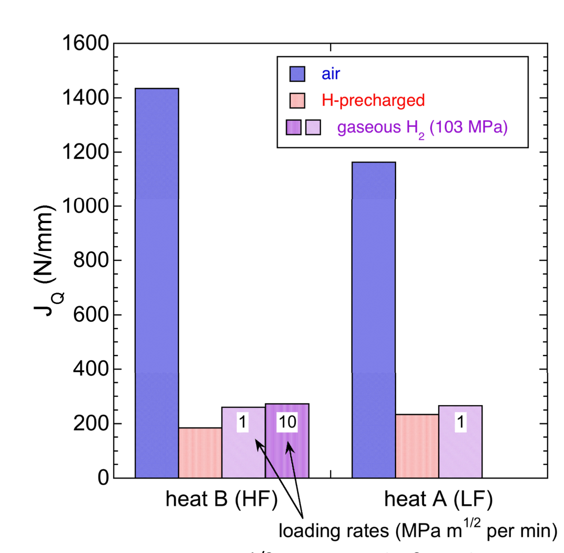

Note: 220 MPa $m^{1/2}$ = 224 kJ/m^2 (N/mm)

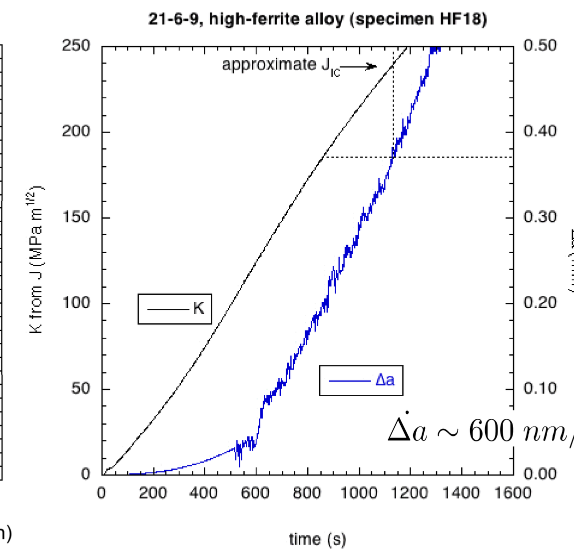

$\dot{\Delta a} \sim 600\ nm/s$

- Fracture toughness degrades with increasing helium concentrations
- Both tritium and helium are requisite for degradation
- Transition from void evolution to fracture along twin and grain boundaries

Morgan and Tosten, Tritium and decay helium effects on the fracture toughness, International Conference on Hydrogen (1994)

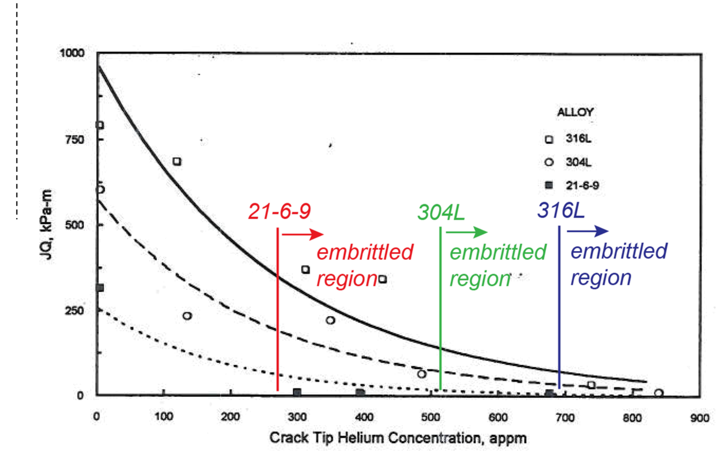

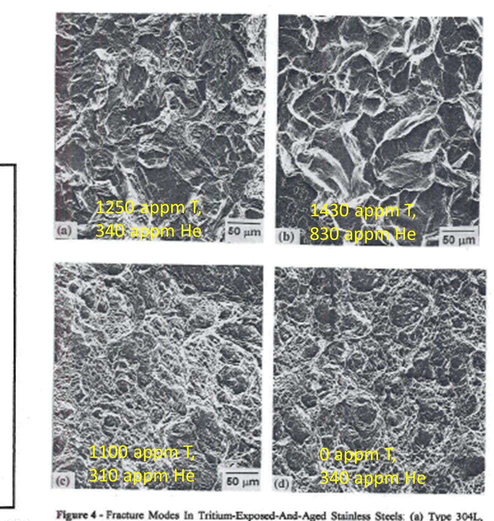

Figure 4 - Fracture Modes In Tritium-Exposed-And-Aged Stainless Steels: (a) Type 304L, 1250 Tritium, 340 appm He; (b) Type 304L, 1430 Appm Tritium, 830 appm He; (c) Type 316L Steel 1100 appm Tritium 310 appm He; (d) Type 304L, Tritium Degassed, ~ 0 appm T, 340 appm He.

This path heavily leverages Sofronis/McMeeking (1989)* and Krom (1998).
Recent work by Leo and Anand (2013).

Transport of hydrogen in the current configuration

$$D^*\dot{c}_l + C^*\mathrm{div}\boldsymbol{v} - \nabla_{\boldsymbol{x}} \cdot \boldsymbol{d}_l \nabla_{\boldsymbol{x}} c_l - \nabla_{\boldsymbol{x}} \cdot \frac{c_l}{J}\boldsymbol{d}_l \nabla_{\boldsymbol{x}} J + \nabla_{\boldsymbol{x}} \cdot \frac{c_l V_H}{RT}\boldsymbol{d}_l \nabla_{\boldsymbol{x}} \tau_h + \frac{\theta_l}{J}\frac{\partial N_T}{\partial \epsilon_p}\dot{\epsilon}_p - \frac{\theta_t N_T}{J^2}\dot{J} = 0$$

Transport of hydrogen in the reference configuration (push back)

$$D^*\dot{C}_L - \nabla_{\boldsymbol{X}} \cdot d_l \boldsymbol{C}^{-1}\nabla_{\boldsymbol{X}} C_L + \nabla_{\boldsymbol{X}} \cdot \frac{d_l V_H}{RT}\boldsymbol{C}^{-1}\nabla_{\boldsymbol{X}} \tau_h C_L + \theta_T \frac{dN_T}{d\epsilon_p}\dot{\epsilon}_p$$

transient term — *diffusion term* — *advection term from hydrostatic stress* — *source term from trapping*

Deformation-dependent diffusivity $\boldsymbol{D}_L = \boldsymbol{F}^{-1}\boldsymbol{d}_l \boldsymbol{F}^{-T} = d_l \boldsymbol{C}^{-1}$

Goal: Capture sub-grid processes through methods that regularize the jump

$$\boldsymbol{F} = \boldsymbol{F}^{\parallel}\boldsymbol{F}^{\perp}$$
$$\boldsymbol{F}^{\parallel} = \boldsymbol{g}_i \otimes \boldsymbol{G}^i$$
$$\boldsymbol{F}^{\perp} = \boldsymbol{I} + \frac{[\![\boldsymbol{\Phi}]\!]}{h} \otimes \boldsymbol{N}$$
$$\boldsymbol{F} = \boldsymbol{F}^{\parallel} + \frac{[\![\boldsymbol{\varphi}]\!]}{h} \otimes \boldsymbol{N}$$

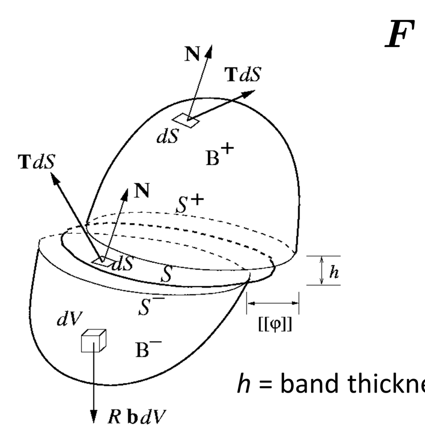

h = band thickness

- Finite-deformation kinematics
- Simulation of strain localization
- No additional constitutive assumptions

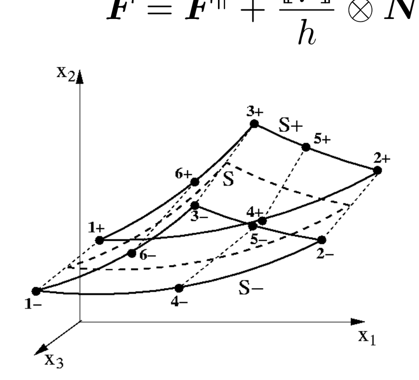

Akin to "cohesive" element

Yang, Mota and Ortiz (IJNME, 2005), Armero and Garikipati (IJSS, 1996)

Fox and Simo (1990), Callari, Armero, Abati (2010)

redefine space $\boldsymbol{X} = \boldsymbol{\Phi}(\xi^1,\xi^2,\xi^3) = \bar{\boldsymbol{\Phi}}(\xi^1,\xi^2) + \boldsymbol{N}(\xi^1,\xi^2)\xi^3$ $\qquad \boldsymbol{G}_i = \boldsymbol{\Phi}_{,i} = \frac{\partial \boldsymbol{X}}{\partial \xi^i}$

include jump in C $C(\boldsymbol{X}) = \bar{C}(\bar{\boldsymbol{\Phi}}[\xi^1,\xi^2]) + \frac{[\![C]\!](\bar{\boldsymbol{\Phi}}[\xi^1,\xi^2])}{h}\xi^3$ $\qquad \nabla_{\boldsymbol{X}} C = (\nabla\boldsymbol{\Phi})^{-T}\frac{\partial C}{\partial \xi^i}$

Finite element implementation is straightforward

$$\nabla_{\boldsymbol{X}} C\big|_{\xi^3=0} = [B]\begin{bmatrix}\{C\}^+\\ \{C\}^-\end{bmatrix} = \begin{bmatrix}[B]^+ & [B]^-\end{bmatrix}\begin{bmatrix}\{C\}^+\\ \{C\}^-\end{bmatrix}$$

$$B^{\pm}_{ia} = \begin{bmatrix}G^1_i & G^2_i & G^3_i\end{bmatrix}\cdot\begin{bmatrix}\frac{1}{2}\frac{\partial N_a}{\partial \xi^1} & \frac{1}{2}\frac{\partial N_a}{\partial \xi^2} & \pm\frac{1}{h}N_a\end{bmatrix}$$

i = # dimensions, *a* = # nodes

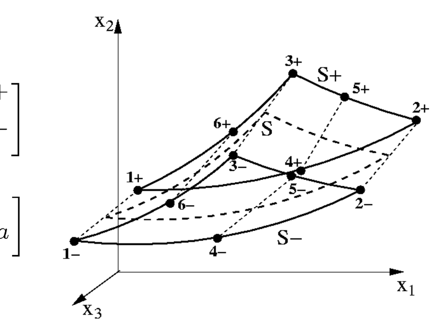

Given this gradient operator, we can use the same PDE for finite-deformation diffusion

$$D^*\dot{C}_L - \nabla_{\boldsymbol{X}} \cdot d_l \boldsymbol{C}^{-1}\nabla_{\boldsymbol{X}} C_L + \nabla_{\boldsymbol{X}} \cdot \frac{d_l V_H}{RT}\boldsymbol{C}^{-1}\nabla_{\boldsymbol{X}} \tau_h C_L + \theta_T \frac{dN_T}{d\epsilon_p}\dot{\epsilon}_p$$

Implementation of fast pathway (no deformation):

$$\int_{\mathcal{B}^G} \nabla_{\boldsymbol{X}} v D_L(\boldsymbol{X})\nabla_{\boldsymbol{X}} C\, dV \approx h\sum_{j=1}^{N^M_{\mathrm{int}}} \overline{W}(\xi^1_j,\xi^2_j)\begin{bmatrix}v^+_a(\xi^1_j,\xi^2_j) & v^-_a(\xi^1_j,\xi^2_j)\end{bmatrix}\begin{bmatrix}\vec{B}^+(\xi^1_j,\xi^2_j)\\ \vec{B}^-(\xi^1_j,\xi^2_j)\end{bmatrix} D_L(\boldsymbol{X}) \begin{bmatrix}\vec{B}^+(\xi^1_j,\xi^2_j) & \vec{B}^-(\xi^1_j,\xi^2_j)\end{bmatrix}\begin{bmatrix}C^+_a\\ C^-_a\end{bmatrix}$$

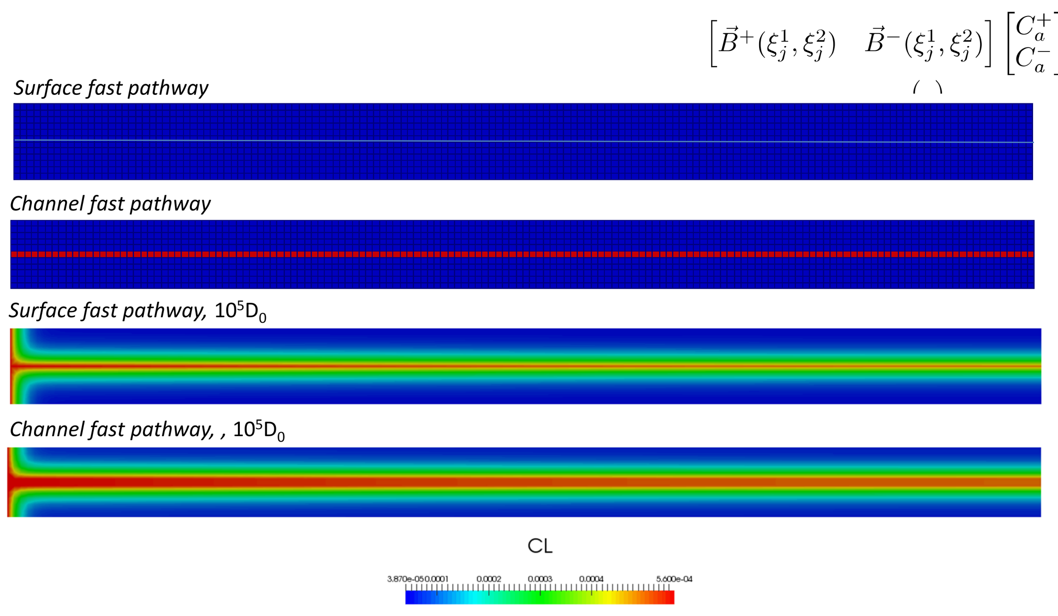

Grain boundary diffusion coupled with mechanical loading:

- Stretched in horizontal direction
- Fast pathway = $10^5 D_0$
- Horizontal diffusion
- Vertical diffusion

$\boldsymbol{D}_L = \boldsymbol{F}^{-1}\boldsymbol{d}_l \boldsymbol{F}^{-T} = d_l \boldsymbol{C}^{-1}$

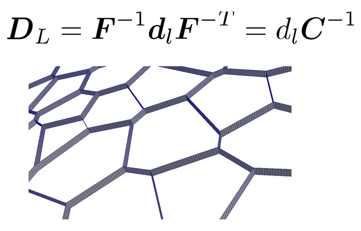

Horizontal diffusion — Vertical diffusion

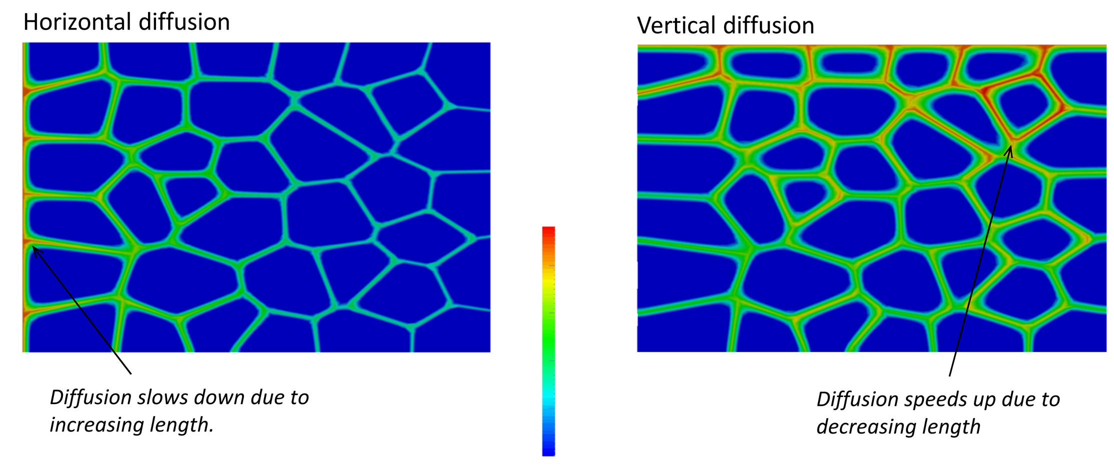

Diffusion slows down due to increasing length.

Diffusion speeds up due to decreasing length

Units are scaled in the balance of linear momentum, conservation of concentration, and L_2 projection to improve condition number of the system

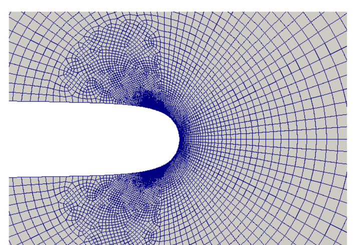

https://software.sandia.gov/albany/

$D^*\dot{C}_L$

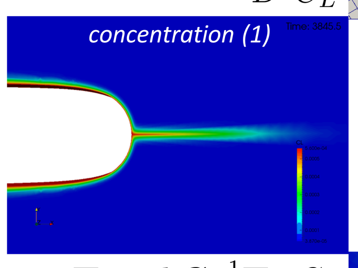

- Path: $10^5 D_0$
- K_{app}: 85 MPa $m^{1/2}$
- Time: 3850 s

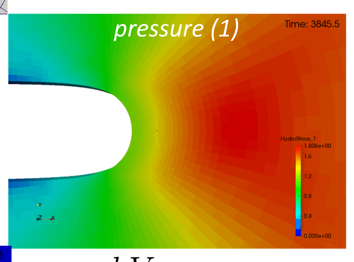

$\nabla_{\boldsymbol{X}} \cdot d_l \boldsymbol{C}^{-1}\nabla_{\boldsymbol{X}} C_L$

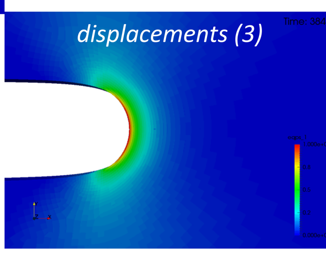

$\nabla_{\boldsymbol{X}} \cdot \frac{d_l V_H}{RT}\boldsymbol{C}^{-1}\nabla_{\boldsymbol{X}} \tau_h C_L$

$+\ \theta_T \frac{dN_T}{d\epsilon_p}\dot{\epsilon}_p$

NOTE: 85 MPa $m^{1/2}$ is well below J_Q for 21Cr-6Ni-9Mn (220 MPa $m^{1/2}$)

We seek to find descriptors of helium bubble formation that result from the radioactive decay of tritium (T) to He.
- Schaldach and Wolfer (2004) focus on the total number of clusters (total bubble density)

1000s of ODEs for helium clusters are condensed into 3 coupled ODEs written in
- Single He (monomers) N_1, total bubble density, N_b, and bubble volume fraction S_b
- ODEs are nonlinear. We can integrate them implicitly with Newton's method
- Chemo-mechanical solution (T, **u**). Solve ODEs (dependent on T) at integration points.

$$\frac{dN_1}{dt} = G(t) - 16\pi(r_1+r_1)DN_1^2 - 4\pi DN_1\left(\frac{3}{4\pi}\right)^{\frac{1}{3}} S_b^{\frac{1}{3}} N_b^{\frac{2}{3}}$$
$$\frac{dN_b}{dt} = 8\pi(r_1+r_1)DN_1^2$$
$$\frac{\eta}{\Omega}\frac{dS_b}{dt} = 16\pi(r_1+r_1)DN_1^2 + 4\pi DN_1\left(\frac{3}{4\pi}\right)^{\frac{1}{3}} S_b^{\frac{1}{3}} N_b^{\frac{2}{3}}$$

$$C_{He} = N_1 + \left(\frac{\eta}{\Omega}\right)S_b$$

G(t) – helium source term
r_1 - initial bubble radius
η - number of He atoms/vacant site
Ω - partial molar volume

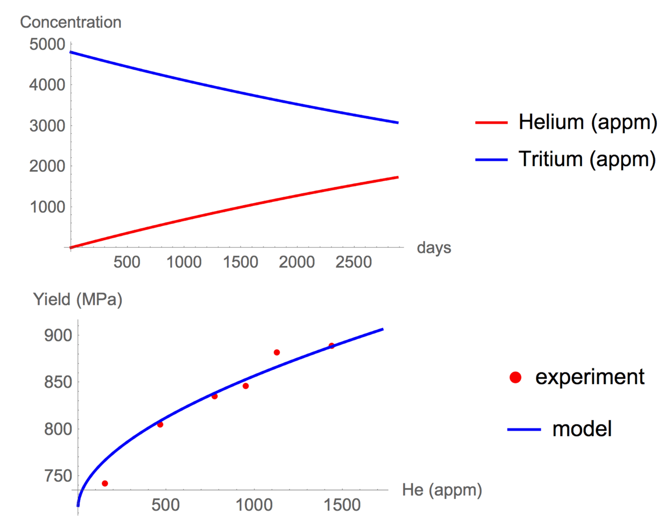

Comparison of current model to experimental data by Robinson and Thomas (1991). Data from hydrogen yields α_1 (hydrogen = tritium). Nonlinearity in fit stems from average bubble radius, not fitting parameter α_2. Both parameters are needed to accurately fit Robinson's data.

From helium bubble ODEs, we have:

N_b total bubble density
S_b bubble volume fraction

Calculate average bubble radius:

$$\bar{R}_b = \left(\frac{3S_b}{4\pi N_b}\right)^{\frac{1}{3}}$$

Assumptions for yield stress σ_y:
- Rate independent yield stress σ_0
- Proportional to T concentration, C_T
- Misfit strengthening from He is dominant (Arsenlis, Wolfer, JNM)
- Misfit strengthening varies w/R_b^2
- Normalize w/He atomic radius R_a

$$Y(C_T,\bar{R}_b) = Y_0 + \alpha_1 C_T + \alpha_2\left(\frac{\bar{R}_b}{R_a}\right)^2$$

α_1 and α_2 are constants fit to experiments

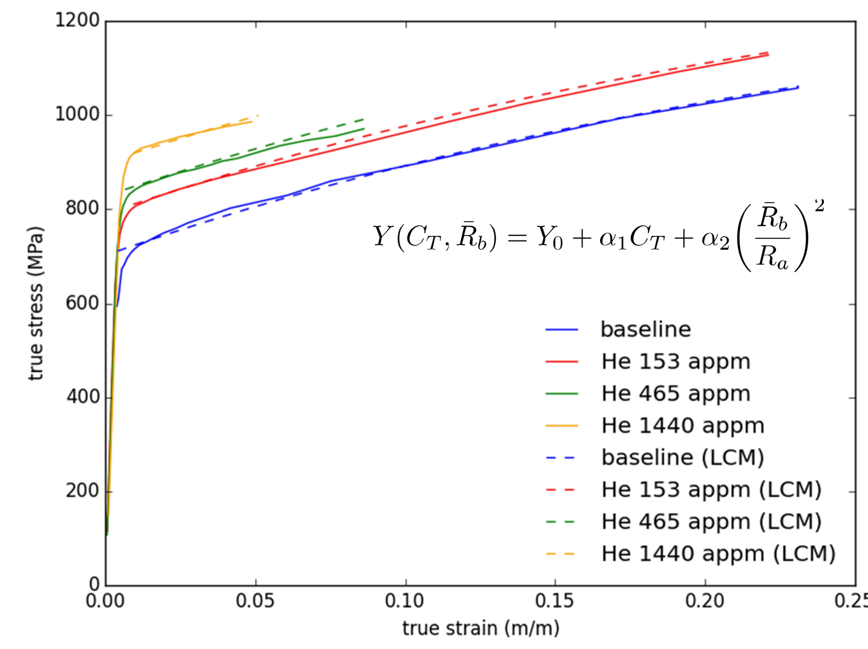

Y_0 = 710 MPa
H = 0.0298μ
R_d = 3.5
α_1 = 63.9 kJ/mol
α_2 = 4.1 MPa

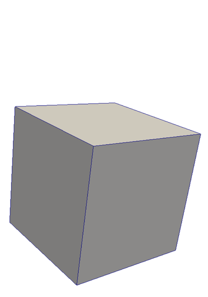

From Robinson and Thomas, "Accelerated Fracture due to Tritium and Helium in 21-6-9 Stainless Steel" (1991). *We cannot locate the source data. Missing He concentrations of 774, 950, and 1128 appm.*

In spirit of Chu and Needleman (1980) we choose an appropriate state variable to capture void nucleation through elevated stresses at pile-ups.

- Void nucleation driven by deformation (dislocations, twins)
  - Tritium C_T hastens process
  - Helium amplifies process
- Void growth through Cocks-Ashby
- Void coalescence governed by S_b
  - Nucleated voids connected by smaller helium bubbles

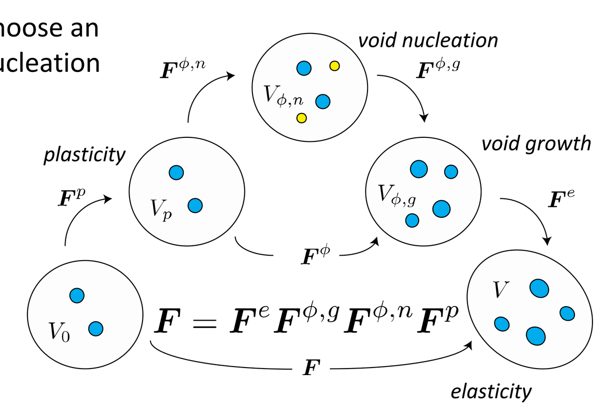

$$\boldsymbol{F} = \boldsymbol{F}^e\boldsymbol{F}^{\phi,g}\boldsymbol{F}^{\phi,n}\boldsymbol{F}^p$$

$$\sigma_y(C_T,R_b) = Y(C_T,R_b) + \kappa \qquad \kappa = 2\mu\epsilon_{ss}$$

$$f_n(\epsilon_{ss},C_T,S_b) = \frac{\phi_{n,\infty}(S_b)}{\sqrt{2\pi}\sigma_{\epsilon_{ss}}}\exp\left[-\frac{1}{2}\left(\frac{\epsilon_{ss}-\mu_{\epsilon_{ss}}(C_T)}{\sigma_{\epsilon_{ss}}}\right)^2\right] \quad \text{void nucleation}$$

$$\phi_n(\epsilon_{ss},C_T,S_b) = \frac{1}{2}\phi_{n,\infty}(S_b)\left[1+\mathrm{erf}\left(\frac{\epsilon_{ss}-\mu_{\epsilon_{ss}}(C_T)}{\sqrt{2}\sigma_{\epsilon_{ss}}}\right)\right] \quad \begin{matrix}\mu_{\epsilon_{ss}}(C_T) = \mu_{\epsilon_{ss},0} - \beta_1 C_T\\ \phi_{n,\infty}(S_b) = \phi_{n,0} + \beta_2 S_B\end{matrix}$$

$$\dot{\phi} = \sqrt{\frac{2}{3}}\dot{\epsilon}_p\frac{1-(1-\phi)^{m+1}}{(1-\phi)^m}\sinh\left[\frac{2(2m-1)}{2m+1}\frac{\langle p\rangle}{\sigma_e}\right] \quad \text{void growth}$$

$$\phi_{coal} = \phi_{coal,0} - \beta_3 S_B \quad \text{void coalescence}$$

Initial constitutive modeling parameters for T/He embrittlement - more work needed

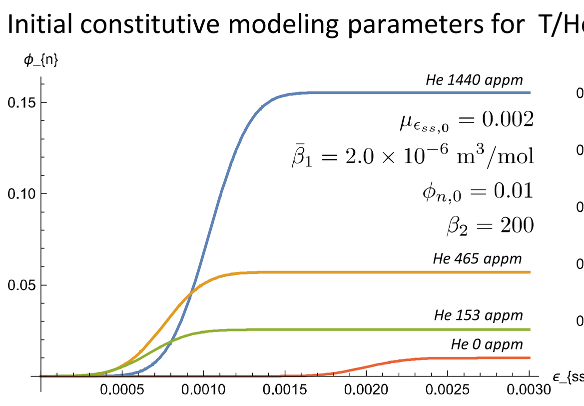

$\mu_{\epsilon_{ss,0}} = 0.002$
$\bar{\beta}_1 = 2.0 \times 10^{-6}\ \mathrm{m^3/mol}$
$\phi_{n,0} = 0.01$
$\beta_2 = 200$

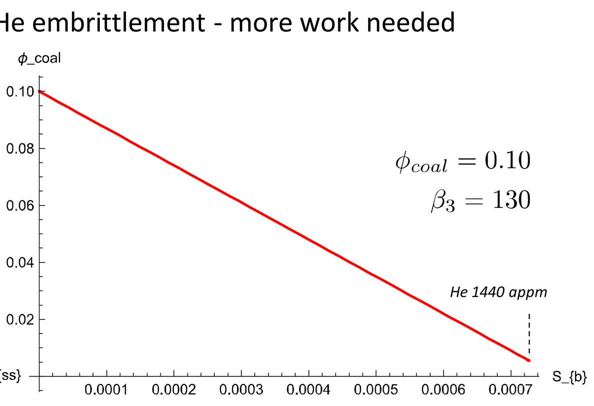

$\phi_{coal} = 0.10$
$\beta_3 = 130$

$$\mu_{\epsilon_{ss}}(C_T) = \mu_{\epsilon_{ss,0}} - \beta_1 C_T \qquad \phi_{n,\infty}(S_b) = \phi_{n,0} + \beta_2 S_B \qquad \phi_{coal} = \phi_{coal,0} - \beta_3 S_B$$

Modeling 21-6-9 tensile geometries given in Robinson and Thomas (1991)

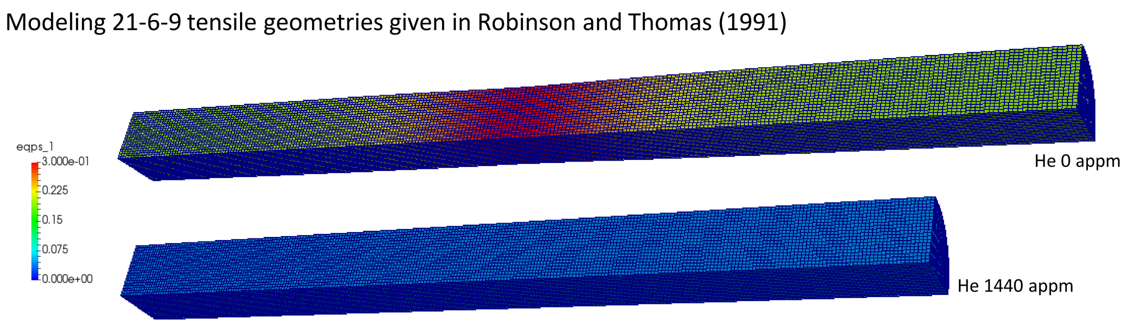

T/He embrittled microstructures can move from nucleation to coalescence

Initial models for void evolution provide a pull for additional experimental data and enable a greater understanding of the crack resistance.

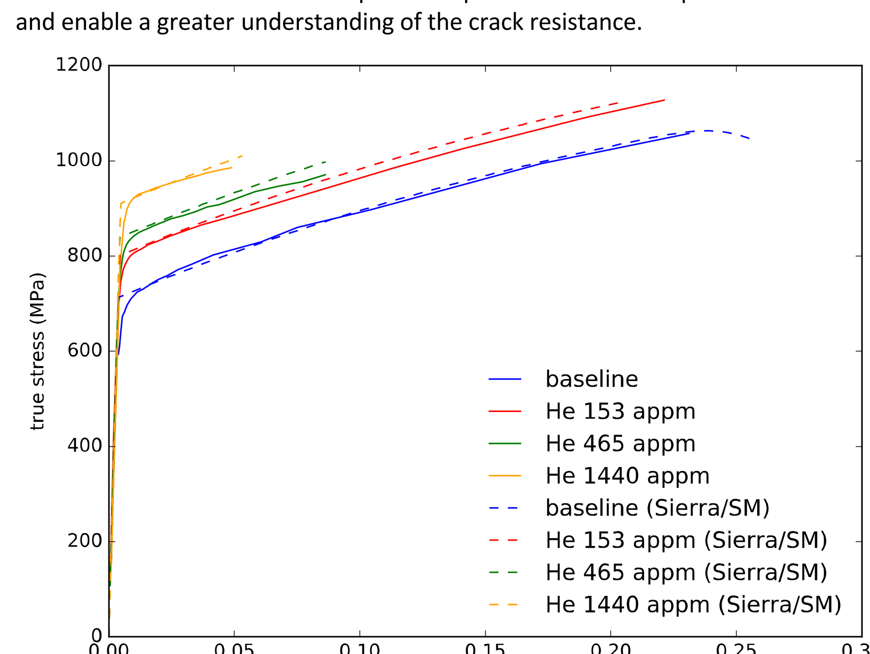

age 1.8 years in tritium
465 appm helium

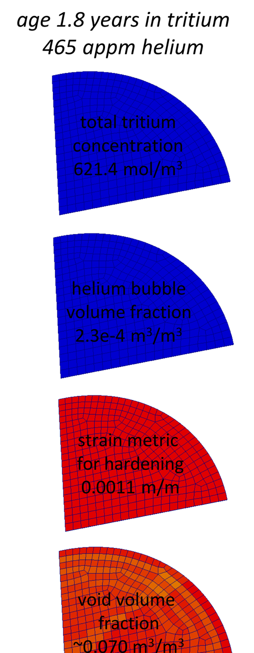

surface elements (1/4 symmetry)

U.S. DEPARTMENT OF ENERGY

National Nuclear Security Administration

Sandia National Laboratories is a multi-program laboratory managed and operated by Sandia Corporation, a wholly owned subsidiary of Lockheed Martin Corporation, for the U.S. Department of Energy's National Nuclear Security Administration under contract DE-AC04-94AL85000.
SAND No. 2011-XXXXP